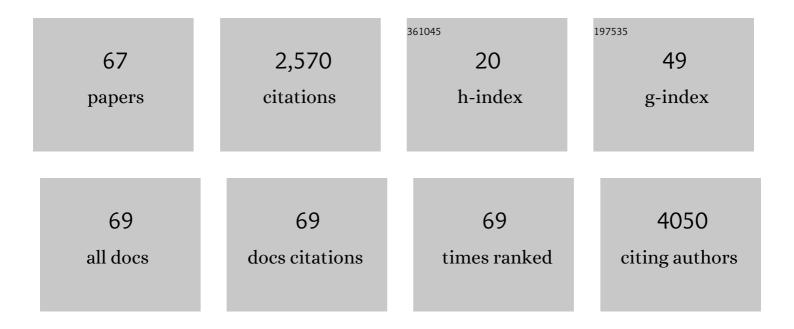
List of Publications by Year in descending order

Source: https://exaly.com/author-pdf/13649/publications.pdf Version: 2024-02-01



#	Article	IF	CITATIONS
1	Clinical recommendations for cardiovascular magnetic resonance mapping of T1, T2, T2* and extracellular volume: A consensus statement by the Society for Cardiovascular Magnetic Resonance (SCMR) endorsed by the European Association for Cardiovascular Imaging (EACVI). Journal of Cardiovascular Magnetic Resonance, 2017, 19, 75.	1.6	1,074
2	MR Evaluation of the Glomerular Homing of Magnetically Labeled Mesenchymal Stem Cells in a Rat Model of Nephropathy. Radiology, 2006, 238, 200-210.	3.6	133
3	Relaxivity of liposomal paramagnetic MRI contrast agents. Magnetic Resonance Materials in Physics, Biology, and Medicine, 2005, 18, 186-192.	1.1	128
4	Feasibility of in vivo15N MRS detection of hyperpolarized 15N labeled choline in rats. Physical Chemistry Chemical Physics, 2010, 12, 5818.	1.3	96
5	Respiratory Self-navigated Postcontrast Whole-Heart Coronary MR Angiography: Initial Experience in Patients. Radiology, 2014, 270, 378-386.	3.6	96
6	Freeâ€running 4D wholeâ€heart selfâ€navigated golden angle MRI: Initial results. Magnetic Resonance in Medicine, 2015, 74, 1306-1316.	1.9	91
7	Serial in vivo MR tracking of magnetically labeled neural spheres transplanted in chronic EAE mice. Magnetic Resonance in Medicine, 2007, 57, 164-171.	1.9	89
8	Free-Breathing 3 T Magnetic Resonance T2-Mapping of the Heart. JACC: Cardiovascular Imaging, 2012, 5, 1231-1239.	2.3	75
9	Selective In Vivo Visualization of Immune-Cell Infiltration in a Mouse Model of Autoimmune Myocarditis by Fluorine-19 Cardiac Magnetic Resonance. Circulation: Cardiovascular Imaging, 2013, 6, 277-284.	1.3	60
10	Hyperpolarized lithiumâ€6 as a sensor of nanomolar contrast agents. Magnetic Resonance in Medicine, 2009, 61, 1489-1493.	1.9	53
11	Selfâ€navigated isotropic threeâ€dimensional cardiac T <sub>2</sub> mapping. Magnetic Resonance in Medicine, 2015, 73, 1549-1554.	1.9	51
12	Fluorine MR Imaging of Inflammation in Atherosclerotic Plaque in Vivo. Radiology, 2015, 275, 421-429.	3.6	50
13	Motion Compensation Strategies in Magnetic Resonance Imaging. Critical Reviews in Biomedical Engineering, 2012, 40, 99-119.	0.5	49
14	Producing over 100ml of highly concentrated hyperpolarized solution by means of dissolution DNP. Journal of Magnetic Resonance, 2008, 194, 152-155.	1.2	39
15	Characterization of perfluorocarbon relaxation times and their influence on the optimization of fluorine-19 MRI at 3 tesla. Magnetic Resonance in Medicine, 2017, 77, 2263-2271.	1.9	25
16	Fluorine-19 Magnetic Resonance Angiography of the Mouse. PLoS ONE, 2012, 7, e42236.	1.1	25
17	Nonâ€invasive quantification of brain glycogen absolute concentration. Journal of Neurochemistry, 2008, 107, 1414-1423.	2.1	24
18	Fluorinated Mesoporous Silica Nanoparticles for Binuclear Probes in <sup>1</sup> H and <sup>19</sup> F Magnetic Resonance Imaging. Langmuir, 2017, 33, 10531-10542.	1.6	21

#	Article	IF	CITATIONS
19	Isotropic threeâ€dimensional <i>T</i> <sub>2</sub> mapping of knee cartilage: Development and validation. Journal of Magnetic Resonance Imaging, 2018, 47, 362-371.	1.9	21
20	Multi-energy photon-counting computed tomography versus other clinical imaging techniques for the identification of articular calcium crystal deposition. Rheumatology, 2021, 60, 2483-2485.	0.9	20
21	Quantification of brain glycogen concentration and turnover through localized <sup>13</sup> C NMR of both the C1 and C6 resonances. NMR in Biomedicine, 2010, 23, 270-276.	1.6	19
22	Chemical shift encoding (CSE) for sensitive fluorineâ€19 MRI of perfluorocarbons with complex spectra. Magnetic Resonance in Medicine, 2018, 79, 2724-2730.	1.9	19
23	Self-Navigation with Compressed Sensing for 2D Translational Motion Correction in Free-Breathing Coronary MRI: A Feasibility Study. PLoS ONE, 2014, 9, e105523.	1.1	17
24	On the accuracy and precision of cardiac magnetic resonance T <sub>2</sub> mapping: A highâ€resolution radial study using adiabatic T <sub>2</sub> preparation at 3 T. Magnetic Resonance in Medicine, 2017, 77, 159-169.	1.9	16
25	Relaxivity of Gd-based contrast agents on X nuclei with long intrinsic relaxation times in aqueous solutions. Magnetic Resonance Imaging, 2007, 25, 821-825.	1.0	15
26	Hyperpolarized <sup>6</sup> Li as a probe for hemoglobin oxygenation level. Contrast Media and Molecular Imaging, 2016, 11, 41-46.	0.4	15
27	Noncontrast free-breathing respiratory self-navigated coronary artery cardiovascular magnetic resonance angiography at 3 T using lipid insensitive binomial off-resonant excitation (LIBRE). Journal of Cardiovascular Magnetic Resonance, 2019, 21, 38.	1.6	15
28	Ultra-high-resolution 3D imaging of atherosclerosis in mice with synchrotron differential phase contrast: a proof of concept study. Scientific Reports, 2015, 5, 11980.	1.6	14
29	Endogenous assessment of myocardial injury with single-shot model-based non-rigid motion-corrected T1 rho mapping. Journal of Cardiovascular Magnetic Resonance, 2021, 23, 119.	1.6	14
30	Fat signal suppression for coronary MRA at 3T using a waterâ€selective adiabatic T <sub>2</sub> â€preparation technique. Magnetic Resonance in Medicine, 2014, 72, 763-769.	1.9	13
31	Three-Dimensional Self-Navigated T2 Mapping for the Detection of Acute Cellular Rejection After Orthotopic Heart Transplantation. Transplantation Direct, 2017, 3, e149.	0.8	12
32	Simultaneous fatâ€free isotropic 3D anatomical imaging and T <sub>2</sub> mapping of knee cartilage with lipidâ€insensitive binomial offâ€resonant RF excitation (LIBRE) pulses. Journal of Magnetic Resonance Imaging, 2019, 49, 1275-1284.	1.9	11
33	Scalable Learning-Based Sampling Optimization for Compressive Dynamic MRI. , 2020, , .		11
34	Combined T <sub>2</sub> â€preparation and twoâ€dimensional pencilâ€beam inner volume selection. Magnetic Resonance in Medicine, 2015, 74, 529-536.	1.9	10
35	A chemical shift encoding (CSE) approach for spectral selection in fluorineâ€19 MRI. Magnetic Resonance in Medicine, 2018, 79, 2183-2189.	1.9	10
36	Towards Quantification of Inflammation in Atherosclerotic Plaque in the Clinic – Characterization and Optimization of Fluorine-19 MRI in Mice at 3 T. Scientific Reports, 2019, 9, 17488.	1.6	10

#	Article	IF	CITATIONS
37	Quantification of myocardial interstitial fibrosis and extracellular volume for the detection of cardiac allograft vasculopathy. International Journal of Cardiovascular Imaging, 2020, 36, 533-542.	0.7	10
38	The Road Toward Reproducibility of Parametric Mapping of the Heart: A Technical Review. Frontiers in Cardiovascular Medicine, 2022, 9, .	1.1	10
39	A comparison of in vivo <sup>13</sup> C MR brain glycogen quantification at 9.4 and 14.1 T. Magnetic Resonance in Medicine, 2012, 67, 1523-1527.	1.9	9
40	A characterization of ABLâ€101 as a potential tracer for clinical fluorineâ€19 MRI. NMR in Biomedicine, 2020, 33, e4212.	1.6	9
41	Compressed sensing with signal averaging for improved sensitivity and motion artifact reduction in fluorineâ€19 MRI. NMR in Biomedicine, 2021, 34, e4418.	1.6	8
42	Accelerated and highâ€resolution cardiac <scp>T</scp> <sub>2</sub> mapping through peripheral kâ€space sharing. Magnetic Resonance in Medicine, 2019, 81, 220-233.	1.9	6
43	A blackâ€blood ultraâ€ <b>s</b> hort echo time (UTE) sequence for 3D isotropic resolution imaging of the lungs. Magnetic Resonance in Medicine, 2019, 81, 3808-3818.	1.9	6
44	Cardiac magnetic resonance imaging with T2 mapping for the monitoring of acute heart transplant rejection in patients with problematic endomyocardial biopsy: in anticipation of new recommendations. Kardiologia Polska, 2021, 79, 339-343.	0.3	4
45	Repositioning precision of coronary arteries measured on X-ray angiography and its implications for coronary MR angiography. Journal of Magnetic Resonance Imaging, 2015, 41, 1251-1258.	1.9	3
46	Improved respiratory selfâ€navigation for 3D radial acquisitions through the use of a pencilâ€beam 2Dâ€T <sub>2</sub> â€prep for freeâ€breathing, wholeâ€heart coronary MRA. Magnetic Resonance in Medicine, 2018, 79, 1293-1303.	1.9	3
47	In vitro optimization and comparison of CT angiography versus radial cardiovascular magnetic resonance for the quantification of cross-sectional areas and coronary endothelial function. Journal of Cardiovascular Magnetic Resonance, 2019, 21, 11.	1.6	3
48	Respiratory Motion-Registered Isotropic Whole-Heart T2 Mapping in Patients With Acute Non-ischemic Myocardial Injury. Frontiers in Cardiovascular Medicine, 2021, 8, 712383.	1.1	3
49	Accelerated and KWIC-filtered cardiac T2 mapping for improved precision: proof of principle. Journal of Cardiovascular Magnetic Resonance, 2015, 17, .	1.6	2
50	A robust broadband fatâ€suppressing phaser T 2 â€preparation module for cardiac magnetic resonance imaging at 3T. Magnetic Resonance in Medicine, 2021, 86, 1434-1444.	1.9	2
51	T2 Mapping from Super-Resolution-Reconstructed Clinical Fast Spin Echo Magnetic Resonance Acquisitions. Lecture Notes in Computer Science, 2020, , 114-124.	1.0	2
52	Standards for writing Society for Cardiovascular Magnetic Resonance (SCMR) endorsed guidelines, expert consensus, and recommendations: a report of the publications committee. Journal of Cardiovascular Magnetic Resonance, 2021, 23, 129.	1.6	2
53	Free-breathing T2 mapping at 3T for the monitoring of cardiac allograft rejection: initial results. Journal of Cardiovascular Magnetic Resonance, 2014, 16, M11.	1.6	1
54	Oxygen-sensitive Magnetic Resonance Imaging: A Noninvasive Step Forward for Diagnosing Vasculopathy in the Cardiac Allograft. Transplantation, 2021, 105, 1664-1665.	0.5	1

#	Article	IF	CITATIONS
55	The Cardiomyocyte in Heart Failure with Preserved Ejection Fraction—Victim of Its Environment?. Cells, 2022, 11, 867.	1.8	1
56	Quantitative free-breathing 3T T2-mapping of the heart designed for longitudinal studies. Journal of Cardiovascular Magnetic Resonance, 2012, 14, .	1.6	0
57	Improved fat signal suppression for coronary MRA at 3T using a water-selective adiabatic T2-Prep technique. Journal of Cardiovascular Magnetic Resonance, 2013, 15, O5.	1.6	0
58	Self-navigated three-dimensional cardiac T2 mapping at 3T. Journal of Cardiovascular Magnetic Resonance, 2013, 15, P51.	1.6	0
59	Fat signal suppression for coronary MRA at 3T using a water-selective adiabatic T2-preparation technique. Magnetic Resonance in Medicine, 2014, 72, spcone-spcone.	1.9	0
60	Numerically optimized radiofrequency pulses for robust and low-power cardiovascular T2 preparation at 3T. Journal of Cardiovascular Magnetic Resonance, 2014, 16, P41.	1.6	0
61	Radial cardiac T2 mapping with alternating T2 preparation intrinsically introduces motion correction. Journal of Cardiovascular Magnetic Resonance, 2014, 16, P28.	1.6	0
62	Apparent Diffusion coefficient (ADC), T1 and T2 quantitative indexes of the myocardium in athletes before, during and after extreme mountain ultra-marathon: correlation with myocardial damages and inflammation biomarkers. Journal of Cardiovascular Magnetic Resonance, 2016, 18, O41.	1.6	0
63	Breath-held high-resolution cardiac T2 mapping with SKRATCH. Journal of Cardiovascular Magnetic Resonance, 2016, 18, P27.	1.6	0
64	Initial experience with isotropic 3D cardiac T2 mapping for the monitoring of cardiac allograft rejection. Journal of Cardiovascular Magnetic Resonance, 2016, 18, W23.	1.6	0
65	Isotropic three-dimensional T2 mapping of knee cartilage with T2-prepared segmented gradient ECHO at 3T. Osteoarthritis and Cartilage, 2016, 24, S300-S301.	0.6	0
66	T2 Relaxation Time Varies Within the Load-Bearing Regions of Non-OA Femoral Cartilage. Osteoarthritis and Cartilage, 2017, 25, S249-S250.	0.6	0
67	Chapter 7 Cardiac Disease. , 2016, , 191-220.		0